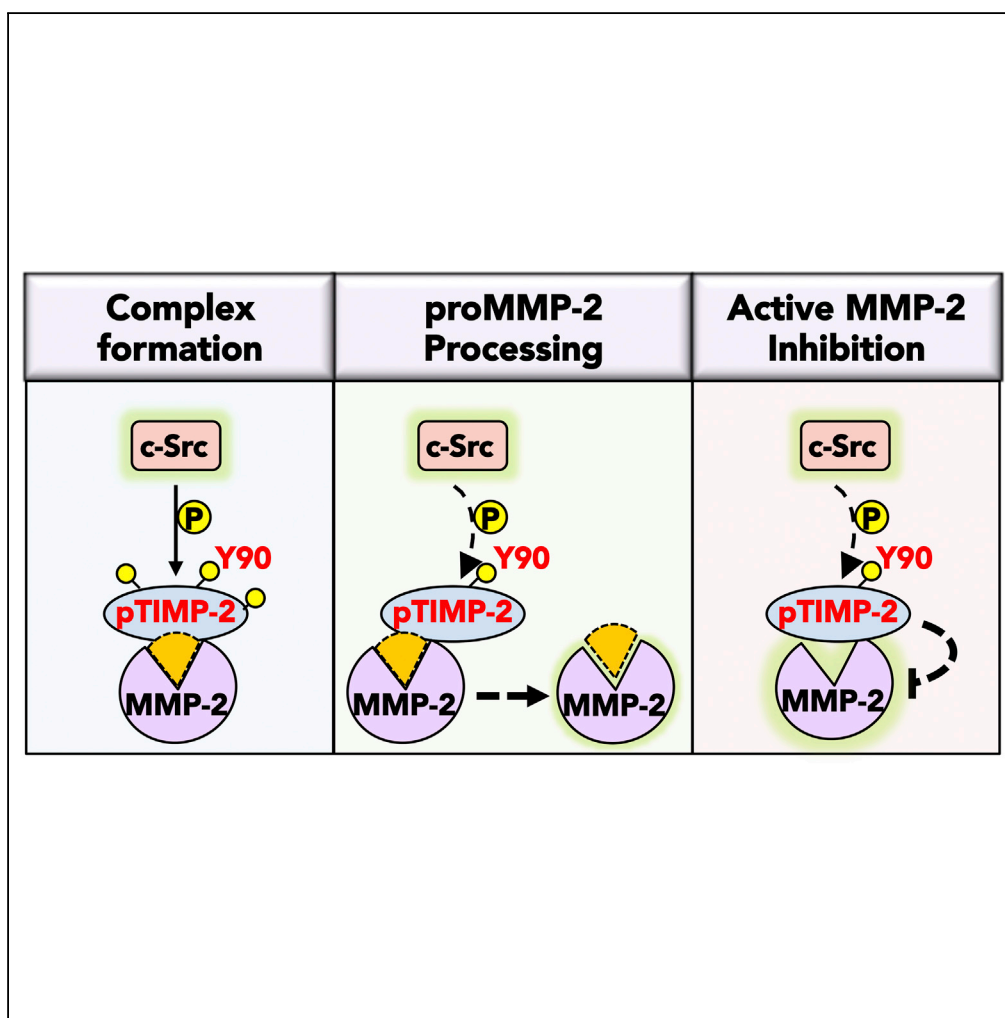


Article

Extracellular Phosphorylation of TIMP-2 by Secreted c-Src Tyrosine Kinase Controls MMP-2 Activity



Javier Sánchez-Pozo, Alexander J. Baker-Williams, Mark R. Woodford, ..., William G. Stetler-Stevenson, Gennady Bratslavsky, Dimitra Bourboulia

bourmpod@upstate.edu

HIGHLIGHTS

c-Src tyrosine kinase phosphorylates TIMP-2

Secreted c-Src phosphorylates TIMP-2 extracellularly

TIMP-2 Y90 phosphorylation promotes extracellular interaction with proMMP-2

Tyrosine phosphorylation of TIMP-2 regulates proMMP-2 processing and MMP-2 activity

Sánchez-Pozo et al., *iScience* 1, 87–96
 March 23, 2018 © 2018 The Author(s).
<https://doi.org/10.1016/j.isci.2018.02.004>

Article

Extracellular Phosphorylation of TIMP-2 by Secreted c-Src Tyrosine Kinase Controls MMP-2 Activity

Javier Sánchez-Pozo,^{1,2,3,5} Alexander J. Baker-Williams,^{1,2,3,5} Mark R. Woodford,^{1,2,3} Renee Bullard,^{1,2} Beiyang Wei,⁴ Mehdi Mollapour,^{1,2,3} William G. Stetler-Stevenson,⁴ Gennady Bratslavsky,^{1,3} and Dimitra Bourboulia^{1,2,3,6,*}

SUMMARY

The tissue inhibitor of metalloproteinases 2 (TIMP-2) is a specific endogenous inhibitor of matrix metalloproteinase 2 (MMP-2), which is a key enzyme that degrades the extracellular matrix and promotes tumor cell invasion. Although the TIMP-2:MMP-2 complex controls proteolysis, the signaling mechanism by which the two proteins associate in the extracellular space remains unidentified. Here we report that TIMP-2 is phosphorylated outside the cell by secreted c-Src tyrosine kinase. As a consequence, phosphorylation at Y90 significantly enhances TIMP-2 potency as an MMP-2 inhibitor and weakens the catalytic action of the active enzyme. TIMP-2 phosphorylation also appears to be essential for its interaction with the latent enzyme proMMP-2 *in vivo*. Absence of the kinase or non-phosphorylatable Y90 abolishes TIMP-2 binding to the latent enzyme, ultimately hampering proMMP-2 activation. Together, TIMP-2 phosphorylation by secreted c-Src represents a critical extracellular regulatory mechanism that controls the proteolytic function of MMP-2.

INTRODUCTION

The tissue inhibitor of metalloproteinases 2 (TIMP-2) belongs to a family of secreted proteins, the TIMPs, that consists of four members (TIMP-1, -2, -3, and -4). TIMPs inhibit the proteolytic activity of a large family of zinc-dependent endopeptidases, the matrix metalloproteinases (MMPs; Brew and Nagase, 2010; Murphy, 2011). MMPs are implicated in the processing of cell surface protein components and in the degradation of constituents of the extracellular matrix (Bourboulia and Stetler-Stevenson, 2010; Kessenbrock et al., 2010). Consequently, TIMPs are essential in maintaining tissue homeostasis while regulating pericellular and interstitial tissue proteolysis during tissue repair and in diseases such as cancer.

MMP-2 is one of the most studied MMPs, mainly because increased protein expression and hyperactivity correlate with tumor development and progression (Egeblad and Werb, 2002). The MMP-2 proteolytic activity is regulated at several levels, including latent proenzyme activation and active site interaction with the inhibitors TIMPs. Interestingly, TIMP-2 also regulates the activation process of latent proMMP-2 through a mechanism that requires TIMP-2 binding to the C terminus of the proenzyme independent from the active site (Strongin et al., 1995; Visse and Nagase, 2003). Although TIMP-2 binding to proMMP-2 is essential for proMMP-2 activation, the mechanism that promotes this crucial interaction between TIMP-2 and MMP-2 is largely unknown. Furthermore, studies have identified phosphorylation sites on certain TIMPs and MMPs; however, the molecular mechanisms and functional significance of these modifications are unclear (Hornbeck et al., 2015; Sariahmetoglu et al., 2007; Williams and Coppolino, 2011).

In this study, we describe a new mechanism that regulates MMP-2 proteolytic function through phosphorylation of TIMP-2 by secreted c-Src tyrosine kinase. We show that c-Src phosphorylates TIMP-2 and initiates a signaling cascade that triggers the extracellular association of TIMP-2 with latent proMMP-2. Site-specific mutagenesis of TIMP-2 Y90 elucidates the functional role of this phosphorylation on TIMP-2 as a potent MMP-2 inhibitor and establishes an extracellular process that controls proMMP-2 activation.

¹Department of Urology, SUNY Upstate Medical University, 750 East Adams Street, Syracuse, NY 13210, USA

²Department of Biochemistry and Molecular Biology, SUNY Upstate Medical University, 750 East Adams Street, Syracuse, NY 13210, USA

³Upstate Cancer Center, SUNY Upstate Medical University, 750 East Adams Street, Syracuse, NY 13210, USA

⁴Radiation Oncology Branch, Center for Cancer Research, National Cancer Institute, 9000 Rockville Pike, Bethesda, MD 20892, USA

⁵These authors contributed equally

⁶Lead Contact

*Correspondence:

bourmpod@upstate.edu

<https://doi.org/10.1016/j.isci.2018.02.004>



RESULTS

c-Src Tyrosine Kinase Phosphorylates TIMP-2

To determine whether endogenous TIMP-2 is tyrosine phosphorylated, we isolated naturally secreted TIMP-2 from serum-free cell-conditioned media (CM) of HT1080 human fibrosarcoma cells (Figure 1A). Following SDS-PAGE, we probed with an anti-pan-phosphotyrosine antibody (phos-Tyr, 4G10) and showed that TIMP-2 is tyrosine phosphorylated (Figure 1A and Table S1. [Information of antibodies used]). To identify which tyrosine residue(s) is(are) subject to phosphorylation, we individually mutated all seven of them to the non-phosphorylatable phenylalanine (F) (Figure 1B, Table S2. [Generated constructs] and Table S3. [Sequences of TIMP-2 constructs]; Betts and Russell, 2003). C-terminal His₆-tagged phosphodeficient mutants, wild type (WT), and vector control (Vec) were transiently expressed in human embryonic kidney 293H (HEK293H) cells. Following pulldown Ni-NTA from cell extracts, we confirmed that WT TIMP-2 is tyrosine phosphorylated (Figure 1C). Moreover, we detected selective phosphorylation at Y62, Y90, and Y165, as demonstrated from the decreased band intensity of the non-phosphorylatable mutants (Y62F, Y90F, and Y165F) compared with WT TIMP-2 control (Figure 1C). We verified phosphorylation at Y62 as previously reported in mass spectrometry-based proteomic data (Hornbeck et al., 2015). We next simultaneously mutated all three tyrosine residues to F, creating the non-phosphorylatable triple mutant Y62F/Y90F/Y165F (referred to as TF). Following pulldown from HEK293H CM, the single mutants had decreased tyrosine phosphorylation, whereas no detectable phosphorylation was seen in the TF mutant (Figure 1D). These data demonstrate that secreted TIMP-2 is tyrosine phosphorylated and that this post-translational modification selectively occurs at residues Y62, Y90, and Y165.

To determine the tyrosine kinase responsible for this phosphorylation, we hypothesized that phosphorylation occurs at key sequence motifs surrounding the targeted residues. Amino acid isoleucine (I) at the $n - 1$ position of Y62 and Y90 ($n + 1$ for Y165) is a common denominator in peptides recognized by c-Src or c-Abl tyrosine kinases (Hubbard and Till, 2000; Pinna and Ruzzene, 1996; Songyang and Cantley, 1995; Figure S1A). To assess TIMP-2 phosphorylation by either tyrosine kinase, we performed an *in vitro* kinase assay using recombinant unphosphorylated TIMP-2-His₆ (rTIMP-2-His₆; Figure 1E). Following pulldown Ni-NTA, we found that c-Src and more intensely v-Src phosphorylate rTIMP-2-His₆ (Figure 1E). v-Src is known to represent the hyperactive oncogenic version of c-Src because of its truncated inhibitory C-terminal regulatory phosphorylation site (Y527; Roskoski, 2004). We quantitatively measured and confirmed the hyperactivity of v-Src used here (Figure S1B). We also found that c-Abl tyrosine kinase did not phosphorylate TIMP-2 (Figure 1E), and in control experiments using heat shock protein 90 alpha (Hsp90 α) as substrate we demonstrate discriminatory phosphorylation by Src kinase but not for c-Abl, confirming our previous work (Beebe et al., 2013; Dunn et al., 2015; Mollapour et al., 2010; Figures 1E and S1C).

To test the *in vivo* phosphorylation of TIMP-2, we transiently expressed WT TIMP-2-His₆ and mutants in a triple kinase knockout (c-Src, Yes, and Fyn) mouse embryonic fibroblast cell line SYF and in cells with wild-type c-Src reintroduced (SYF + c-Src; Figure 1F). Pulldown experiments confirmed tyrosine phosphorylation of WT TIMP-2 in the SYF + c-Src but not in the parental SYF cell CM (Figure 1F). Since phosphorylation at Y62F, Y90F, and Y165F is reduced, and TF lacks phosphorylation in the SYF + c-Src CM, the overall findings suggest that c-Src targets all three tyrosine residues.

Secreted c-Src Phosphorylates TIMP-2 in the Extracellular Space

TIMP-2 contains an amino-terminal signal sequence that directs the newly synthesized protein to the ER, followed by secretion via the ER/Golgi pathway (Benham, 2012; Figure S1A). c-Src is a cytosolic kinase known to phosphorylate substrates at sites localized within the cell. To elucidate the cellular compartment where c-Src phosphorylates TIMP-2, we first assessed c-Src secretion from cells. CM was collected from mammalian cell lines and following normalization to total cellular protein levels, samples were analyzed by immunoblotting (Figures S2A and S2B). c-Src protein was present at varying levels in the extracts and CM from all cell lines tested (Figures S2A and S2B). Absence of cytosolic GAPDH in the CM also verifies lack of cytoplasmic fractions as a result of cell injury. Next, we asked if TIMP-2 could have been phosphorylated before secretion. HEK293H cells were transiently transfected with WT TIMP-2-His₆, followed by 12-hr serum starvation and treatment with brefeldin A, an inhibitor that blocks conventional secretion by disrupting protein transport from ER to Golgi (Figure 2A). As expected, brefeldin A hindered TIMP-2 secretion but not the secretion of c-Src (Figure 2A). Tyrosine phosphorylation was also abolished in TIMP-2 isolated from cell extracts (Figure 2A). These data indicate that tyrosine phosphorylation occurs following TIMP-2 transport to Golgi or extracellularly. As c-Src secretion remains unaffected, we hypothesized that the

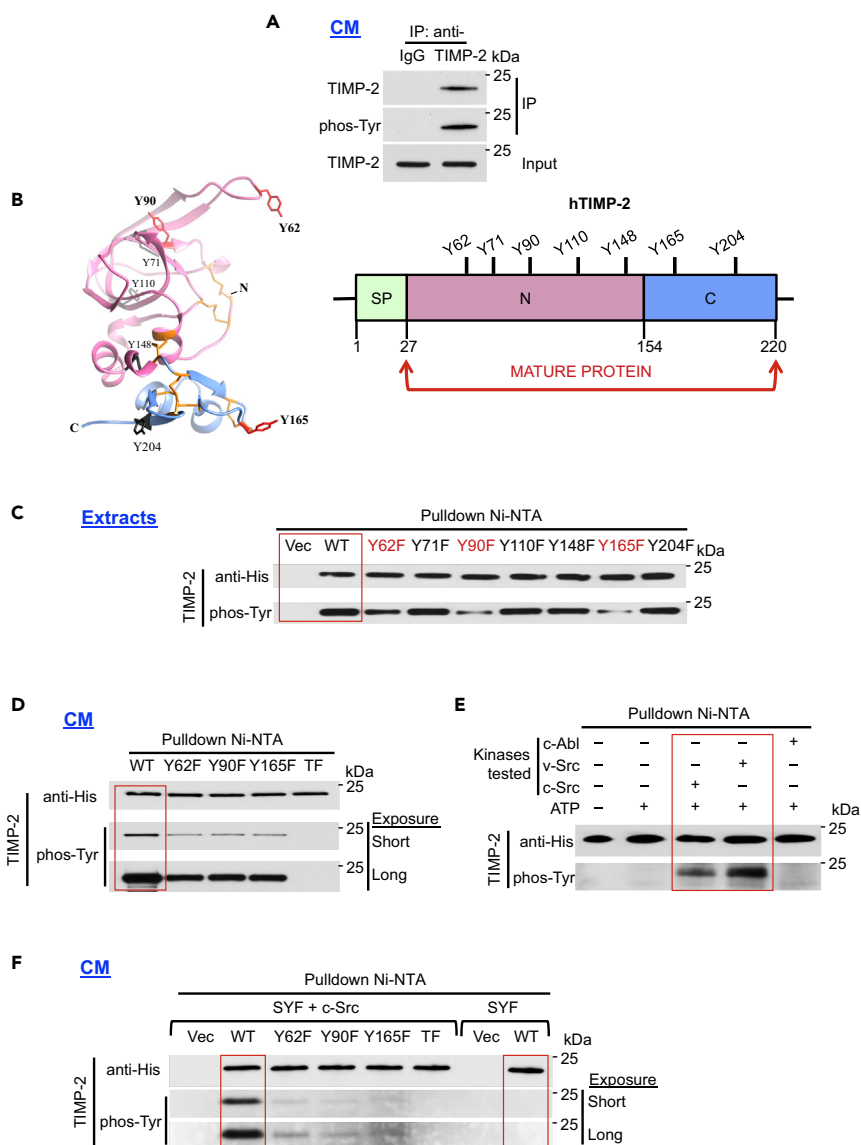


Figure 1. c-Src Phosphorylates Human TIMP-2 *In Vitro* and *In Vivo*

(A) Endogenous secreted TIMP-2 was immunoprecipitated from 10X concentrated HT1080 cell-conditioned media (CM) using anti-TIMP-2 or IgG (control) and analyzed by immunoblotting for phosphorylation using an anti-pan-phosphotyrosine antibody (phos-Tyr, 4G10).

(B) 3D (PDB: 1BR9) and linear domain structures of human TIMP-2 (hTIMP-2). All seven TIMP-2 tyrosine residues (Y) (black) are shown. Numbering is based on the full-length protein sequence (aa 1–220).

(C and D) (C) TIMP-2 His₆-tagged wild type (WT), vector control (Vec), and individual mutant plasmids were transiently expressed in HEK293H cells and pulled down from cell extracts (D) or CM and immunoblotted with indicated antibodies to assess phosphorylation.

(E) Recombinant (rTIMP-2-His₆) was used as the substrate in an *in vitro* kinase assay in the presence of full-length c-Src, v-Src, or c-Abl tyrosine kinases. Following pull-down, immunoblotting was performed to assess tyrosine phosphorylation using phos-Tyr, 4G10 antibody.

(F) TIMP-2 constructs were transiently expressed in SYF and SYF + c-Src cells, pulled down from 10X concentrated CM and immunoblotted to determine TIMP-2 tyrosine phosphorylation.

See also Figure S1.

phosphorylation occurs following secretion. To test this, we serum starved HT1080 cells for 18 hr and then supplemented the CM with rTIMP-2-His₆ (Figure 2B). We detected both TIMP-2 and c-Src in the CM, 2 and 8 hr post treatment (Figure 2B). Notably, the exogenously added rTIMP-2-His₆ is also detected in cell

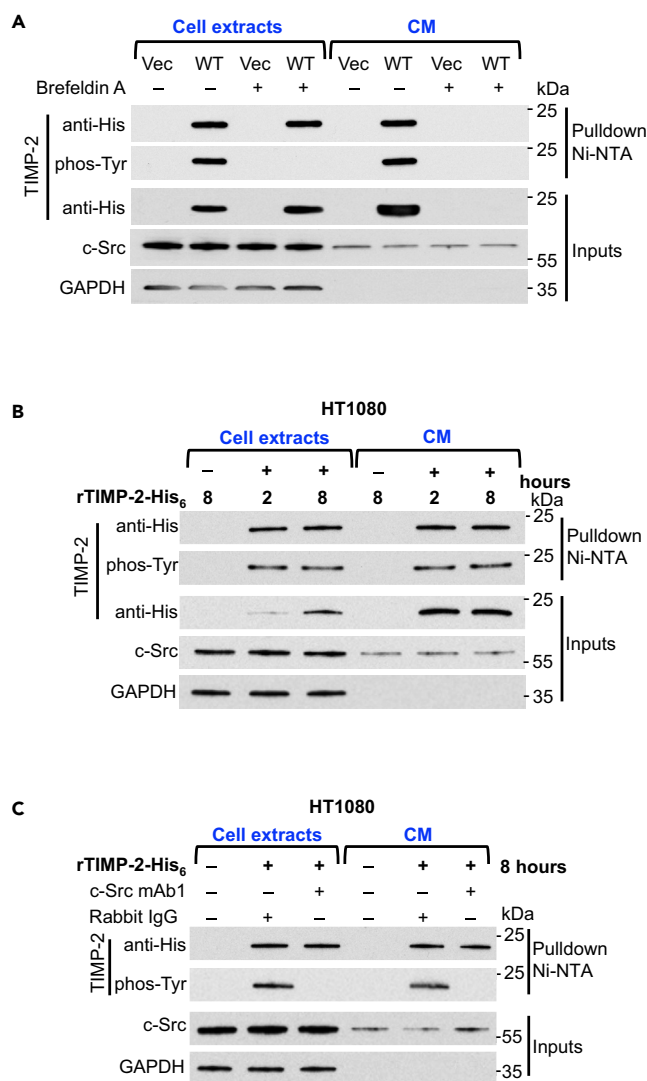


Figure 2. c-Src Phosphorylates TIMP-2 Extracellularly

(A) HEK293H cells were transiently transfected with vector (Vec) control or wild-type (WT) TIMP-2-His₆. Cells were serum starved in the presence (+) and absence (-) of brefeldin A for 12 hr, and cell extracts and CM were collected for immunoblotting and pulldown Ni-NTA to determine c-Src secretion and tyrosine phosphorylation of TIMP-2.

(B) HT1080 cells were serum starved for 24 hr and then treated with rTIMP-2-His₆ for 2 and 8 hr. Cell extracts and CM were collected for immunoblotting and pulldown Ni-NTA analyses to determine phosphorylation of TIMP-2.

(C) Anti-c-Src monoclonal antibody (mAb1) or Rabbit IgG control were added in the CM for 1 hr before addition of recombinant TIMP-2-His₆ for 8 hr. Cell extracts and CM were collected for analyses. GAPDH was analyzed for equal loading in all blots.

See also [Figure S2](#).

extracts, with protein levels increasing over time, indicating that a certain amount of free rTIMP-2-His₆ becomes cell associated ([Figure 2B](#)). It is, therefore, not surprising to find that both cell-associated and free TIMP-2 are tyrosine phosphorylated ([Figure 2B](#)). To strengthen our findings on extracellular phosphorylation, we assessed the effects of anti-c-Src antibodies as possible inhibitors of TIMP-2 tyrosine phosphorylation ([Table S1](#). [Information of antibodies used]). We pre-treated HT1080 cultures with an anti-c-Src antibody (mAb1) or rabbit IgG control before the addition of rTIMP-2-His₆. As predicted, TIMP-2 tyrosine phosphorylation was impaired in both cell extracts and the CM ([Figure 2C](#)). Taken together, our data suggest that TIMP-2 and c-Src are secreted through different secretory pathways and that TIMP-2 is phosphorylated by c-Src outside the cell.

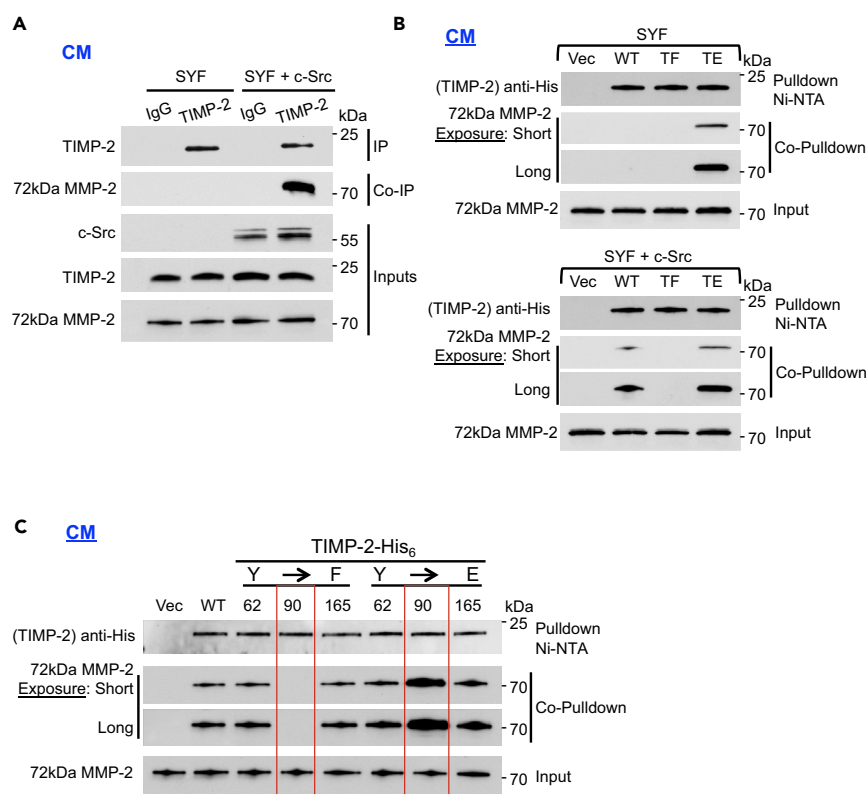


Figure 3. Phosphorylation of Y90 Is Essential for TIMP-2:proMMP-2 Interaction

(A) SYF and SYF + c-Src cells were serum starved for 18 hr. Immunoprecipitation (IP) of endogenous TIMP-2 from the cell CM was followed by co-immunoprecipitation (co-IP) of 72 kDa proMMP-2 to determine interaction.

(B) SYF (top) and SYF + c-Src (bottom) were transiently transfected with Vec control, WT TIMP-2-His₆, and mutants (TF and TE). Pull-down was performed from the CM followed by immunoblotting and co-pull-down to assess protein interaction.

(C) HEK293H cells were transiently transfected with the indicated plasmids. Vec control, WT, and non-phosphorylatable (F) and phosphomimetic (E) TIMP-2 mutants were pulled down from the CM. Interaction of TIMP-2 proteins with secreted 72 kDa proMMP-2 was determined by co-pull-down and immunoblotting.

See also Figure S3.

c-Src-Mediated Phosphorylation of TIMP-2 Y90 Is Essential for Binding to proMMP-2

TIMP-2 interaction with proMMP-2 is crucial for cell surface activation of the latent enzyme (Brown et al., 1993; Morgunova et al., 2002; Strongin et al., 1995; Visse and Nagase, 2003). We next examined if TIMP-2 tyrosine phosphorylation participates in the formation of the proenzyme-inhibitor complex. Using an anti-TIMP-2 antibody we immunoprecipitated endogenous TIMP-2 from SYF CM and found no interaction between TIMP-2 and proMMP-2 (Figure 3A and Table S1. [Information of antibodies used]). In contrast, the TIMP-2:proMMP-2 complex was observed in SYF + c-Src CM by co-immunoprecipitation using anti-TIMP-2 antibody. We next generated and transiently transfected SYF cells with a phosphomimetic triple mutant Y62E/Y90E/Y165E (referred to as TE; Table S2. [Generated constructs], Table S3. [Sequences of TIMP-2 constructs], Table S4. [PCR mutagenesis primer sequences]). In contrast to WT and TF, pull-down of TIMP-2 TE led to co-pull-down of proMMP-2 in the SYF CM (Figure 3B top). Notably, TIMP-2 TE appears to associate more with proMMP-2 than with WT TIMP-2, suggesting that the degree of *in vivo* tyrosine phosphorylation regulates TIMP-2 interaction with MMP-2 (Figures 3B bottom and S3A). As anticipated, WT TIMP-2 from the SYF + c-Src CM also bound to proMMP-2 (Figure 3B bottom). We obtained further evidence from pull-down experiments performed in transiently transfected HEK293H cells and in SYF and SYF + c-Src cells exogenously treated with rTIMP-2-His₆ (Figures S3A and S3B). Taken together, we show that tyrosine phosphorylation of TIMP-2 is required for its interaction with proMMP-2 *in vivo*.

We next asked if phosphorylation of a single tyrosine residue was essential to promote TIMP-2 complex with proMMP-2. Following transient transfection of HEK293H cells with single mutants, our data revealed

that TIMP-2 Y90F does not complex with endogenous proMMP-2, whereas the phosphomimetic Y90E displayed enhanced interaction with the proenzyme (Figure 3C). Our data suggest that phosphorylation of TIMP-2 Y90 is critical to the regulation of the extracellular interaction of TIMP-2 with proMMP-2.

TIMP-2 Y90 Phosphorylation Regulates MMP-2 Function

The classic model of proMMP-2 activation involves TIMP-2 serving as a scaffold that tethers latent 72 kDa proMMP-2 to the plasma membrane (Brown et al., 1993; Strongin et al., 1995; Visse and Nagase, 2003). A membrane-bound active protease MT1-MMP mediates processing of proMMP-2 that generates the intermediate 64 kDa MMP-2 followed by autocatalysis that results in fully active free 62 kDa MMP-2 (Kinoshita et al., 1998; Strongin et al., 1995). As the interaction between TIMP-2 and proMMP-2 precedes the proteolytic processing of the proenzyme *in vivo* (Brown et al., 1993; Strongin et al., 1995), we predicted that Y90 phosphorylation would be critical in this process. We therefore tested WT TIMP-2-His₆, Y90F, and Y90E proteins for their ability to activate proMMP-2 *in vivo*. Proteins purified from HEK293H CM were verified by Coomassie blue staining for purity and by reverse zymography for their ability to inhibit MMP-2-mediated gelatin degradation (Figures S4A–S4C and Table S5. [Buffer composition]).

We next treated HT1080 cells with the purified proteins to stimulate proMMP-2 activation, following the flow diagram (Figure 4A). Gelatin zymography confirmed that WT TIMP-2 facilitated the activation of proMMP-2, shown by the conversion of the 72 kDa proMMP-2 to the 64 and 62 kDa species (Figure 4B). We also confirmed previous studies showing that at high amounts TIMP-2 inhibits proMMP-2 activation (Caterina et al., 2000; Wang et al., 2000). Similar to WT TIMP-2, Y62F/Y165F (Y90 is readily phosphorylated) and Y90E (phosphomimetic) also assist in zymogen activation. However, TIMP-2 Y90F is unable to promote the activation of proMMP-2 (Figure 4B). Similar to our earlier findings in HEK293H CM, TIMP-2 Y90F and proMMP-2 did not interact in the HT1080 cell CM (Figure 4C and Table S1. [Information of antibodies used]). These data suggest that phosphorylation of TIMP-2 Y90 is critical for TIMP-2:proMMP-2 complex formation and cellular activation of proMMP-2.

Active MMP-2 proteolytic activity is also regulated through direct contact with TIMP-2. We next evaluated the impact of Y90 phosphorylation on TIMP-2 ability to inhibit the 62 kDa active MMP-2. We performed steady-state kinetics on the active protease in the presence of purified WT TIMP-2, Y90F, and 90E. Double-reciprocal Lineweaver-Burk plots verified competitive inhibition (Figures S4D–S4F). The initial velocity (v_o) of substrate cleavage was fit to the Michaelis-Menten kinetic model, and the inhibition constant K_i for each TIMP-2 species was determined using the classic model for tight-binding non-competitive inhibition (Figures 4D–4F). We found that TIMP-2 Y90E inhibits active 62 kDa MMP-2 with a K_i of 0.154×10^{-9} M (154 pM), an almost 5-fold increase in active site inhibition (Figures 4F and 4G). The K_i value shown for WT TIMP-2:62 kDa MMP-2 is also in agreement with previous studies (Willenbrock et al., 1993; Wingfield et al., 1999). These data suggest that phosphorylation of Y90 modulates the binding affinity of the inhibitor to active MMP-2.

DISCUSSION

Phosphorylation is considered as one of the fundamental molecular mechanisms that regulate intracellular events from protein-protein interactions and activity to signal transduction and disease development (Nishi et al., 2011). Here we show that secreted TIMP-2 is tyrosine phosphorylated at three tyrosine residues, two of which (Y62 and Y165) are unique to TIMP-2 protein, suggesting that their phosphorylation could modulate extracellular functions specific for TIMP-2 (Figure 1). We concentrated on tyrosine kinases that recognize consensus phosphorylation sites on their targeted substrates and discovered that c-Src tyrosine kinase phosphorylates TIMP-2 (Figure 1). Anti-c-Src antibodies block phosphorylation, supporting the idea that this process occurs extracellularly (Figure 2). Lack of phosphorylation at Y90 compromises proenzyme processing and activation, likely due to disruption of TIMP-2 interaction with proMMP-2 (Figures 3 and 4). Phosphorylation at Y90 enhances the inhibitory function of TIMP-2 against active MMP-2 that is seemingly mediated by an enhanced affinity reflected in the 5-fold increase in K_i observed for phosphomimetic Y90E TIMP-2 (Figure 4). Combined, these findings support a potential role for c-Src in extracellular signaling and protein function (Figure S4G).

How does phosphorylation of Y90 regulate the interaction between TIMP-2 and proMMP-2? The structures of TIMP-2 and proMMP-2 are already solved, and, indeed, Y90 is located far away from the known interface between the two proteins (Morgunova et al., 2002). However, we believe our current knowledge on the

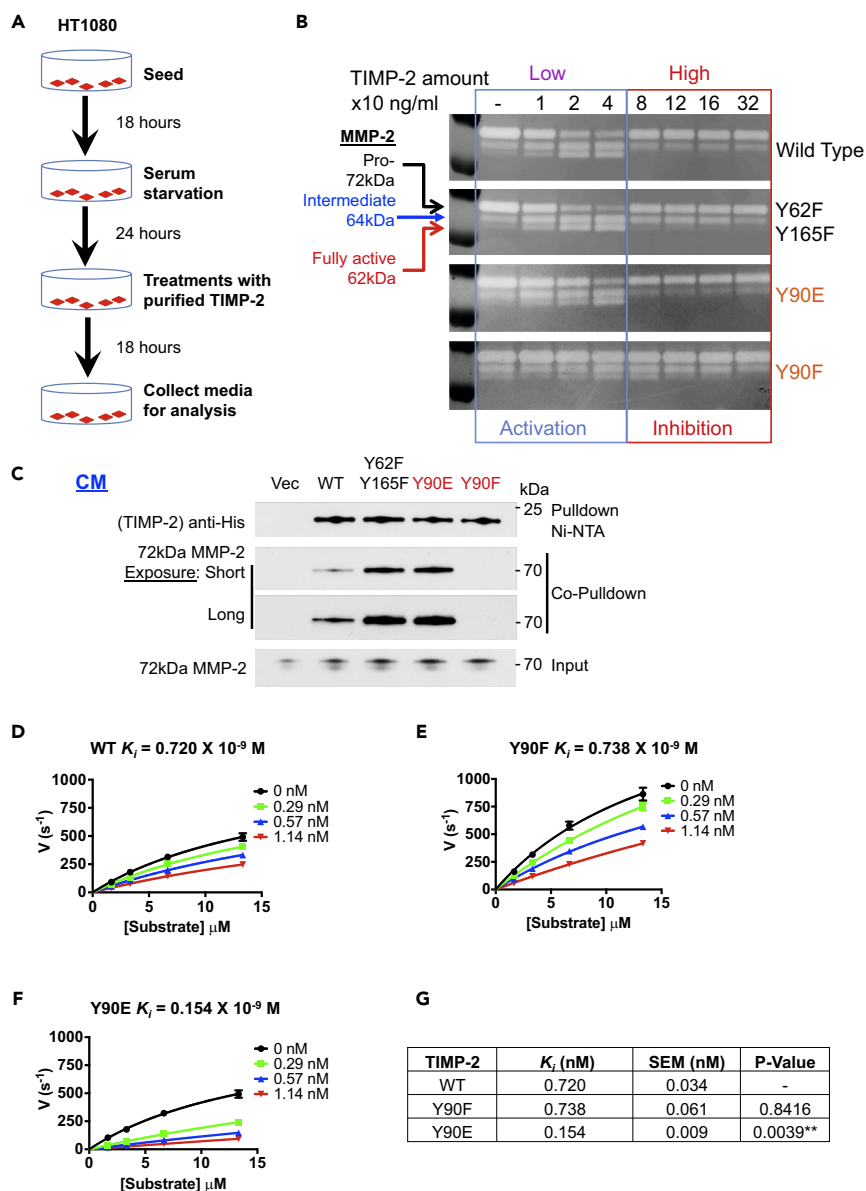


Figure 4. TIMP-2 Tyr90 Regulates MMP-2 Function

(A) Flowchart followed in proMMP-2 activation studies.

(B) HEK293H-purified WT TIMP-2 and indicated mutant proteins were added at increasing concentrations in the CM of HT1080 cells. Media were collected and analyzed by gelatin zymography. MMP-2 forms shown include the 72 kDa proMMP-2, 64 kDa intermediate form, and 62 kDa fully active form. Reduction of the 72 kDa form and increase of the 64 kDa and 62 kDa forms indicate proMMP-2 activation.

(C) TIMP-2-His₆ proteins were transiently transfected in HT1080 cells followed by pull-down and co-pull-down for proMMP-2 to assess protein interaction.

(D–F) HEK293H-purified WT TIMP-2, (E) Y90F, (F) and Y90E were tested for their ability to inhibit active MMP-2. Enzyme and inhibitors were pre-incubated at 25°C for 15 min before substrate addition. Experiments were performed at least twice. Error bars represent mean \pm SD of three technical replicates.

(G) WT TIMP-2, Y90F, and Y90E K_i were determined to assess TIMP-2 inhibitory potency and represent the mean average of at least two independent experiments. A Student's t-test was performed between the WT and each of the two mutants. p Values were estimated to assess statistical significance (**p < 0.01).

See also Figure S4.

structure of free human TIMP-2 or the formation of TIMP-2:proMMP-2 complexes has been largely built upon structural data and biophysical studies, in which bacterial or low eukaryotic expression systems are utilized to produce recombinant proteins devoid of any post-translational modifications (Brew and Nagase, 2010; Morgunova et al., 1999, 2002; Tuuttila et al., 1998). Our data argue that in the extracellular space, protein complexes are dependent upon specific signals, including post-translational modifications, in contrast to the high-affinity protein-protein interactions that readily occur in *in vitro* systems. Furthermore, it is quite possible that in the cellular context, inter-domain or additional local protein interactions that facilitate changes of TIMP-2 structural properties and assist in the binding to proMMP-2 following phosphorylation may take place. Further studies are warranted to address these questions.

Our data also suggest that c-Src kinase mediates the extracellular phosphorylation of TIMP-2. We identified c-Src released in the cell CM, corroborating emerging studies showing that c-Src is enriched in the extracellular vesicles (DeRita et al., 2016; Di Noto et al., 2013). Brefeldin A inhibited TIMP-2 but not c-Src secretion, and ER-retained TIMP-2 appears not to be tyrosine phosphorylated. Although it is possible that the TIMP-2 post-translational modification occurs after protein transport to Golgi (Figure 2A), there is no evidence to support c-Src localization within the Golgi network (Reinecke and Caplan, 2014; Sato et al., 2009). Alternatively, it is possible that both proteins somehow co-localize at the plasma membrane where phosphorylation could take place following their release. Nevertheless, we demonstrated that anti-c-Src antibodies block phosphorylation of exogenous TIMP-2 (Figure 2C).

We determined that latent enzyme processing depends on the phosphorylation of TIMP-2 by c-Src. Our findings that TIMP-2:proMMP-2 interaction is coupled to TIMP-2 tyrosine phosphorylation provides an explanation. TIMP-2 Y90 phosphorylation could support conformational changes exposing interaction surfaces that facilitate favorable and stronger complex formation with proMMP-2 *in vivo* (Batra et al., 2013; Sharabi et al., 2014; Zou et al., 2016). Expression of the phosphomimetic TIMP-2 TE in SYF cells was sufficient to restore TIMP-2 interaction with proMMP-2 (Figure 3B). Lack of TIMP-2 phosphorylation would also hinder activation (Bernardo and Fridman, 2003; Butler et al., 1998; English et al., 2006; Lafleur et al., 2003; Morrison et al., 2001). Indeed, the inability of TIMP-2 Y90F to interact with proMMP-2 was critical for generating the intermediate 64 kDa MMP-2 (Figures 3C, 4B, and 4C). It is also possible that phosphorylation of TIMP-2 may be implicated in MT1-MMP:TIMP-2 complex formation that would change the dynamics of the MT1-MMP:TIMP-2:proMMP-2 complex (Brew and Nagase, 2010; Rapti et al., 2006; Williamson et al., 2001). Thus, the overall mechanism of proMMP-2 activation warrants further investigation.

TIMP-2 also interacts with the active site of MMP-2, resulting in enzyme inhibition (Brew and Nagase, 2010). Structural changes on TIMP-2 Y90E may have increased its affinity for the active site of the enzyme, explaining its lower K_i (Figure 4F). We could also speculate that as TIMP-2 displays biphasic binding for 62 kDa MMP-2, Y90E may bind strongly to the C-terminal domain of active MMP-2 before binding and inhibiting the active site of the enzyme (Olson et al., 1997). Future studies utilizing TIMP-2 phosphomimetics and MMP-2 domain mutants will provide further insight into the role of TIMP-2 phosphorylation in the binding and inhibition of MMP-2.

METHODS

All methods can be found in the accompanying [Transparent Methods supplemental file](#).

SUPPLEMENTAL INFORMATION

Supplemental Information includes Transparent Methods, four figures, and five tables and can be found with this article online at <https://doi.org/10.1016/j.isci.2018.02.004>.

ACKNOWLEDGMENTS

We gratefully acknowledge Dr. Peg AtKisson for providing critical comments on the manuscript. We wish to thank Dr. Paul Soloway for providing us with the MEF TIMP-2 knock-out (TIMP-2 $-/-$ + *ras/myc*) cell line. This work was supported by funds from SUNY Upstate Medical University, The Upstate Foundation, SUNY Research Foundation, and Upstate Breast Cancer Research Funds to D.B. and M.M., The Carol M. Baldwin Research Grant to D.B. and M.M., and Associated Medical Schools of New York to D.B.

AUTHOR CONTRIBUTIONS

Conceptualization, D.B. and M.M.; Methodology, D.B. and M.M.; Investigation, J.S.-P., A.J.B.-W., M.R.W., R.B., B.W., M.M., and D.B.; Writing – Original draft, D.B.; Writing – Review and Editing, J.S.-P., A.J.B.-W., M.M., W.G.S.-S., G.B., and D.B.; Funding Acquisition, M.M. and D.B.; Resources, M.M., W.G.S.-S., G.B., and D.B.; Supervision, D.B.

DECLARATION OF INTERESTS

D.B., M.M., and G.B. have filed for a patent based partially on results presented in this manuscript. The other authors declare no competing interests.

Received: December 19, 2017

Revised: January 29, 2018

Accepted: February 8, 2018

Published: March 23, 2018

REFERENCES

- Batra, J., Soares, A.S., Mehner, C., and Radisky, E.S. (2013). Matrix metalloproteinase-10/TIMP-2 structure and analyses define conserved core interactions and diverse exosite interactions in MMP/TIMP complexes. *PLoS One* 8, e75836.
- Beebe, K., Mollapour, M., Scroggins, B., Prodromou, C., Xu, W., Tokita, M., Taldone, T., Pullen, L., Zierer, B.K., Lee, M.J., et al. (2013). Posttranslational modification and conformational state of heat shock protein 90 differentially affect binding of chemically diverse small molecule inhibitors. *Oncotarget* 4, 1065–1074.
- Benham, A.M. (2012). Protein secretion and the endoplasmic reticulum. *Cold Spring Harb. Perspect. Biol.* 4, a012872.
- Bernardo, M.M., and Fridman, R. (2003). TIMP-2 (tissue inhibitor of metalloproteinase-2) regulates MMP-2 (matrix metalloproteinase-2) activity in the extracellular environment after pro-MMP-2 activation by MT1 (membrane type 1)-MMP. *Biochem. J.* 374, 739–745.
- Betts, M.J., and Russell, R.B. (2003). Amino acid properties and consequences of substitutions. In *Bioinformatics for Geneticists*, M.R. Barnes and I.C. Gray, eds. (John Wiley & Sons, Ltd), pp. 291–316.
- Bourboulia, D., and Stetler-Stevenson, W.G. (2010). Matrix metalloproteinases (MMPs) and tissue inhibitors of metalloproteinases (TIMPs): positive and negative regulators in tumor cell adhesion. *Semin. Cancer Biol.* 20, 161–168.
- Brew, K., and Nagase, H. (2010). The tissue inhibitors of metalloproteinases (TIMPs): an ancient family with structural and functional diversity. *Biochim. Biophys. Acta* 1803, 55–71.
- Brown, P.D., Kleiner, D.E., Unsworth, E.J., and Stetler-Stevenson, W.G. (1993). Cellular activation of the 72 kDa type IV procollagenase/TIMP-2 complex. *Kidney Int.* 43, 163–170.
- Butler, G.S., Butler, M.J., Atkinson, S.J., Will, H., Tamura, T., Schade van Westrum, S., Crabbe, T., Clements, J., d'Ortho, M.P., and Murphy, G. (1998). The TIMP2 membrane type 1 metalloproteinase “receptor” regulates the concentration and efficient activation of
- progelatinase A. A kinetic study. *J. Biol. Chem.* 273, 871–880.
- Caterina, J.J., Yamada, S., Caterina, N.C., Longenecker, G., Holmback, K., Shi, J., Yermovsky, A.E., Engler, J.A., and Birkedal-Hansen, H. (2000). Inactivating mutation of the mouse tissue inhibitor of metalloproteinases-2(Timp-2) gene alters proMMP-2 activation. *J. Biol. Chem.* 275, 26416–26422.
- DeRita, R.M., Zerlanko, B., Singh, A., Lu, H., Iozzo, R.V., Benovic, J.L., and Languino, L.R. (2016). c-Src, insulin-like growth factor I receptor, G-protein-coupled receptor kinases and focal adhesion kinase are enriched into prostate cancer cell exosomes. *J. Cell Biochem.* 118, 66–73.
- Di Noto, G., Paolini, L., Zendrini, A., Radeghieri, A., Caimi, L., and Ricotta, D. (2013). C-src enriched serum microvesicles are generated in malignant plasma cell dyscrasia. *PLoS One* 8, e70811.
- Dunn, D.M., Woodford, M.R., Truman, A.W., Jensen, S.M., Schulman, J., Caza, T., Remillard, T.C., Loiselle, D., Wolfgeher, D., Blagg, B.S.J., et al. (2015). c-Abl mediated tyrosine phosphorylation of Aha1 activates its co-chaperone function in cancer cells. *Cell Rep.* 12, 1006–1018.
- Egeblad, M., and Werb, Z. (2002). New functions for the matrix metalloproteinases in cancer progression. *Nat. Rev. Cancer* 2, 161–174.
- English, J.L., Kassiri, Z., Koskivirta, I., Atkinson, S.J., Di Grappa, M., Soloway, P.D., Nagase, H., Vuorio, E., Murphy, G., and Khokha, R. (2006). Individual Timp deficiencies differentially impact pro-MMP-2 activation. *J. Biol. Chem.* 281, 10337–10346.
- Hornbeck, P.V., Zhang, B., Murray, B., Kornhauser, J.M., Latham, V., and Skrzypek, E. (2015). PhosphoSitePlus, 2014: mutations, PTMs and recalibrations. *Nucleic Acids Res.* 43, D512–D520.
- Hubbard, S.R., and Till, J.H. (2000). Protein tyrosine kinase structure and function. *Annu. Rev. Biochem.* 69, 373–398.
- Kessenbrock, K., Plaks, V., and Werb, Z. (2010). Matrix metalloproteinases: regulators of the tumor microenvironment. *Cell* 141, 52–67.
- Kinoshita, T., Sato, H., Okada, A., Ohuchi, E., Imai, K., Okada, Y., and Seiki, M. (1998). TIMP-2 promotes activation of progelatinase A by membrane-type 1 matrix metalloproteinase immobilized on agarose beads. *J. Biol. Chem.* 273, 16098–16103.
- Lafleur, M.A., Tester, A.M., and Thompson, E.W. (2003). Selective involvement of TIMP-2 in the second activation cleavage of pro-MMP-2: refinement of the pro-MMP-2 activation mechanism. *FEBS Lett.* 553, 457–463.
- Mollapour, M., Tsutsumi, S., Donnelly, A.C., Beebe, K., Tokita, M.J., Lee, M.J., Lee, S., Morra, G., Bourboulia, D., Scroggins, B.T., et al. (2010). Swe1Wee1-dependent tyrosine phosphorylation of Hsp90 regulates distinct facets of chaperone function. *Mol. Cell* 37, 333–343.
- Morgunova, E., Tuuttila, A., Bergmann, U., Isupov, M., Lindqvist, Y., Schneider, G., and Tryggvason, K. (1999). Structure of human pro-matrix metalloproteinase-2: activation mechanism revealed. *Science* 284, 1667–1670.
- Morgunova, E., Tuuttila, A., Bergmann, U., and Tryggvason, K. (2002). Structural insight into the complex formation of latent matrix metalloproteinase 2 with tissue inhibitor of metalloproteinase 2. *Proc. Natl. Acad. Sci. USA* 99, 7414–7419.
- Morrison, C.J., Butler, G.S., Bigg, H.F., Roberts, C.R., Soloway, P.D., and Overall, C.M. (2001). Cellular activation of MMP-2 (gelatinase A) by MT2-MMP occurs via a TIMP-2-independent pathway. *J. Biol. Chem.* 276, 47402–47410.
- Murphy, G. (2011). Tissue inhibitors of metalloproteinases. *Genome Biol.* 12, 233.
- Nishi, H., Hashimoto, K., and Panchenko, A.R. (2011). Phosphorylation in protein-protein binding: effect on stability and function. *Structure* 19, 1807–1815.
- Olson, M.W., Gervasi, D.C., Mobashery, S., and Fridman, R. (1997). Kinetic analysis of the binding of human matrix metalloproteinase-2 and -9 to

tissue inhibitor of metalloproteinase (TIMP)-1 and TIMP-2. *J. Biol. Chem.* 272, 29975–29983.

Pinna, L.A., and Ruzzene, M. (1996). How do protein kinases recognize their substrates? *Biochim. Biophys. Acta* 1314, 191–225.

Rapti, M., Knauper, V., Murphy, G., and Williamson, R.A. (2006). Characterization of the AB loop region of TIMP-2. Involvement in pro-MMP-2 activation. *J. Biol. Chem.* 281, 23386–23394.

Reinecke, J., and Caplan, S. (2014). Endocytosis and the Src family of non-receptor tyrosine kinases. *Biomol. Concepts* 5, 143–155.

Roskoski, R., Jr. (2004). Src protein-tyrosine kinase structure and regulation. *Biochem. Biophys. Res. Commun.* 324, 1155–1164.

Sariahmetoglu, M., Crawford, B.D., Leon, H., Sawicka, J., Li, L., Ballermann, B.J., Holmes, C., Berthiaume, L.G., Holt, A., Sawicki, G., et al. (2007). Regulation of matrix metalloproteinase-2 (MMP-2) activity by phosphorylation. *FASEB J.* 21, 2486–2495.

Sato, I., Obata, Y., Kasahara, K., Nakayama, Y., Fukumoto, Y., Yamasaki, T., Yokoyama, K.K., Saito, T., and Yamaguchi, N. (2009). Differential trafficking of Src, Lyn, Yes and Fyn is specified by the state of palmitoylation in the SH4 domain. *J. Cell Sci.* 122, 965–975.

Sharabi, O., Shirian, J., Grossman, M., Lebendiker, M., Sagi, I., and Shifman, J. (2014).

Affinity- and specificity-enhancing mutations are frequent in multispecific interactions between TIMP2 and MMPs. *PLoS One* 9, e93712.

Songyang, Z., and Cantley, L.C. (1995). Recognition and specificity in protein tyrosine kinase-mediated signalling. *Trends Biochem. Sci.* 20, 470–475.

Strongin, A.Y., Collier, I., Bannikov, G., Marmer, B.L., Grant, G.A., and Goldberg, G.I. (1995). Mechanism of cell surface activation of 72-kDa type IV collagenase. Isolation of the activated form of the membrane metalloprotease. *J. Biol. Chem.* 270, 5331–5338.

Tuuttila, A., Morgunova, E., Bergmann, U., Lindqvist, Y., Maskos, K., Fernandez-Catalan, C., Bode, W., Tryggvason, K., and Schneider, G. (1998). Three-dimensional structure of human tissue inhibitor of metalloproteinases-2 at 2.1 Å resolution. *J. Mol. Biol.* 284, 1133–1140.

Visse, R., and Nagase, H. (2003). Matrix metalloproteinases and tissue inhibitors of metalloproteinases: structure, function, and biochemistry. *Circ. Res.* 92, 827–839.

Wang, Z., Juttermann, R., and Soloway, P.D. (2000). TIMP-2 is required for efficient activation of proMMP-2 in vivo. *J. Biol. Chem.* 275, 26411–26415.

Willenbrock, F., Crabbe, T., Slocombe, P.M., Sutton, C.W., Docherty, A.J., Cockett, M.I., O'Shea, M., Brocklehurst, K., Phillips, I.R., and Murphy, G. (1993). The activity of the tissue

inhibitors of metalloproteinases is regulated by C-terminal domain interactions: a kinetic analysis of the inhibition of gelatinase A. *Biochemistry* 32, 4330–4337.

Williams, K.C., and Coppolino, M.G. (2011). Phosphorylation of membrane type 1-matrix metalloproteinase (MT1-MMP) and its vesicle-associated membrane protein 7 (VAMP7)-dependent trafficking facilitate cell invasion and migration. *J. Biol. Chem.* 286, 43405–43416.

Williamson, R.A., Hutton, M., Vogt, G., Rapti, M., Knauper, V., Carr, M.D., and Murphy, G. (2001). Tyrosine 36 plays a critical role in the interaction of the AB loop of tissue inhibitor of metalloproteinases-2 with matrix metalloproteinase-14. *J. Biol. Chem.* 276, 32966–32970.

Wingfield, P.T., Sax, J.K., Stahl, S.J., Kaufman, J., Palmer, I., Chung, V., Corcoran, M.L., Kleiner, D.E., and Stetler-Stevenson, W.G. (1999). Biophysical and functional characterization of full-length, recombinant human tissue inhibitor of metalloproteinases-2 (TIMP-2) produced in *Escherichia coli*. Comparison of wild type and amino-terminal alanine appended variant with implications for the mechanism of TIMP functions. *J. Biol. Chem.* 274, 21362–21368.

Zou, H., Wu, Y., and Brew, K. (2016). Thermodynamic basis of selectivity in the interactions of tissue inhibitors of metalloproteinases N-domains with matrix Metalloproteinases-1, -3, and -14. *J. Biol. Chem.* 291, 11348–11358.

ISCI, Volume 1

Supplemental Information

Extracellular Phosphorylation of TIMP-2

by Secreted c-Src Tyrosine Kinase

Controls MMP-2 Activity

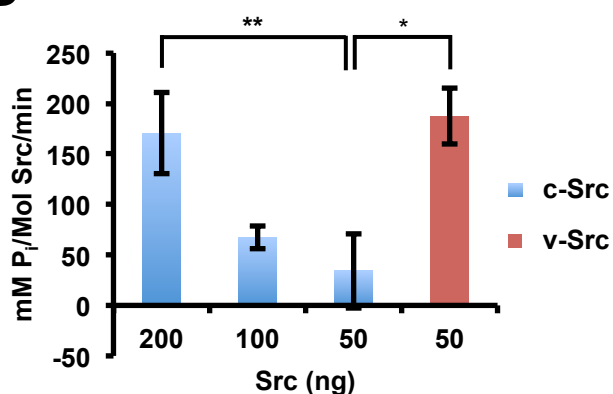
Javier Sánchez-Pozo, Alexander J. Baker-Williams, Mark R. Woodford, Renee Bullard, Beiyang Wei, Mehdi Mollapour, William G. Stetler-Stevenson, Gennady Bratslavsky, and Dimitra Bourboulia

Figure S1

A

	← Signal peptide (TIMP-2, aa 1-26) →	--- N-term ---→	
TIMP-1	MAPFE---PLASGILLLLWLIAPSR---	ACTCVPPHPQTAF CNSDLVIRAKFVGTPEVNQ	54
TIMP-2	MGAAARTLRLALGLLLLATLLRP---	ADACSCSPVHPQQAFCNADVIRAKAVSEKEVDS	57
TIMP-3	M-----TPWLGLIVLLGSWSLGDWG-	AEACTCSPSHPQDAFCNSDIVIRAKVVGKKLVKE	54
TIMP-4	MPGSPRPAPSWVLLLLRLLALLRPPGLGEACSCAPAH	PQQHICH SALLVIRAKISSEKVVPA	60
	* * * * * * * * * * * * * * * * * *		
	Y62	Y90	
TIMP-1	TT-----LYQR Y EIKMTKMYKGFQALGDAADIRFVYTPAMESVCGYFHRSHNRSEEF	L	107
TIMP-2	GNDI Y GNPIKRIQ Y EIKQIKMFKG--PE---KDIEFI Y TAPSSAVCGVSLDV-GGKKEYL		111
TIMP-3	G-----PFGTLV Y TIKQMKMYRGFTKM---PHVQYI Y HTEASESLCGLKLEV-N-KYQYL		103
TIMP-4	SADP-ADTEKMLR Y EIKQIKMFKGFQK---KDVQYI Y TPFDSSLCGVKLEA-NSQKQYL		115
	* * * * * * * * * * * * * * * *	C-term	
		Y165 →	
TIMP-1	IAGKLQ-DGLLHITTCFVAPWNSLSLAQRRGFTK Y TVGCEECTVFPCLSIPCKLQSGT		166
TIMP-2	IAGKAEGDGKMHITLCDFIVPWDLSTTQKKS Y LHRYQMGCE-CKITRCPMIPCYISSPD		170
TIMP-3	LTGRVY-DGKMYTGLCNFVERWDQLTLSQRKGLNRY Y HLGCN-CKIKSCYYLPCFVTSKN		161
TIMP-4	LTGQVLSDGKVF Y IHLN Y IEPWEDLSLVQRESLN Y HLNCG-CQITTCYTPCTISAPN		174
	* * * * * * * * * * * * * * * * * * * *		
TIMP-1	HCLWTDQLLQSGSEKGFQSRHLACLPREPGLCTWQSLRSQIA-----		207
TIMP-2	ECLWMDWVTEK Y NINGHQAKFFACIKRSDGSCAWYRGAAPPKQEFLDIEDP		220
TIMP-3	ECLWTDMLSNFGYPGYQSKHYACIRQKGGYCSWYRGWAPPDKSIINATDP		211
TIMP-4	ECLWTDWLLERKLYGYQAQHYVCMKHVDGTC Y RGHPLRKEFVDIVQP		224
	* * * * * * * * * * * * * * * * * *		

B



C

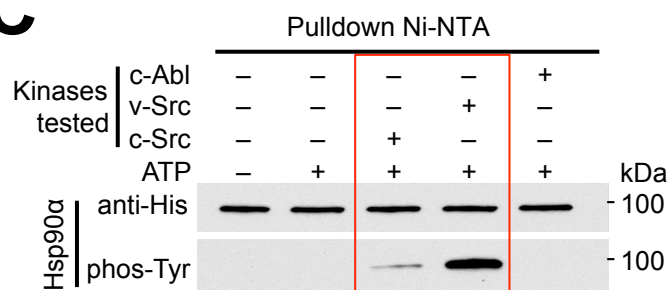


Figure S1. [Alignment of human TIMPs protein family and *in vitro* kinase assay], Related to Figure 1

(A) Protein sequence alignment (ClustalW) of full length human TIMPs (TIMP-1 to -4). Asterisks (*) indicate conserved amino acid residues. Tyrosine residues (Y) subjected to phosphorylation are highlighted in red and tyrosine residues not targeted for phosphorylation are outlined in red.

(B) *In vitro* kinase activity of recombinant c-Src-GST and v-Src-GST tyrosine kinases as determined by measuring the amount of free inorganic phosphate in solution released for each active kinase in the presence of ATP. The experiment was carried out in duplicate. All the data represent mean \pm SD. A Student's *t*-test was performed to assess statistical significance (* $P < 0.05$ and ** $P < 0.005$).

(C) *In vitro* kinase assay to determine human Hsp90 α phosphorylation by tested kinases. Hsp90 α -His₆ pulldown and immunoblotting were performed to assess Hsp90 α tyrosine phosphorylation using anti-His (for Hsp90 α) and anti-pan-phos-Tyr antibodies.

Figure S2

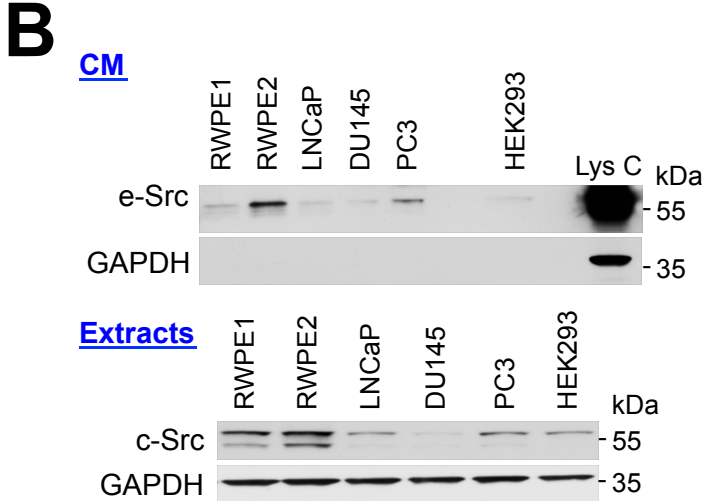
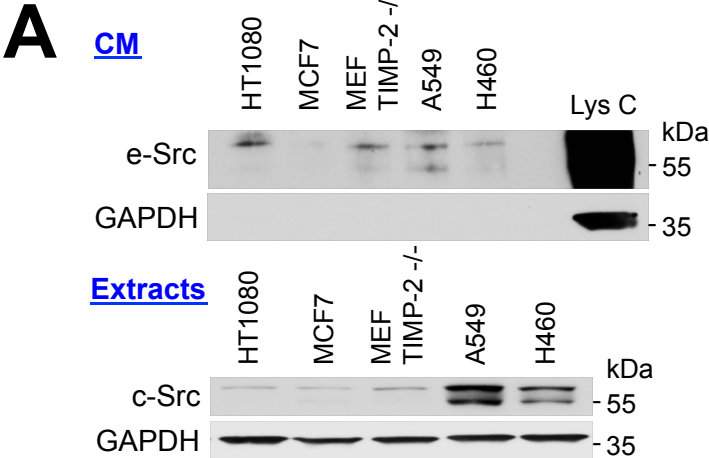


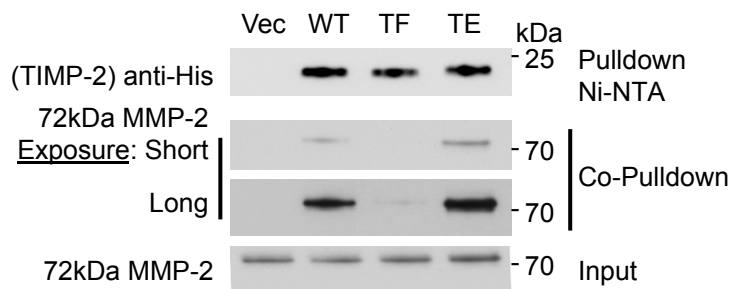
Figure S2. [c-Src tyrosine kinase is present in cell conditioned media], Related to Figure 2

(A) Conditioned media (CM) and cell extracts were collected from human fibrosarcoma HT1080, human breast cancer MCF7, mouse embryonic fibroblasts MEF TIMP-2^{-/-} ras/myc, human lung cancer A549 and H460;

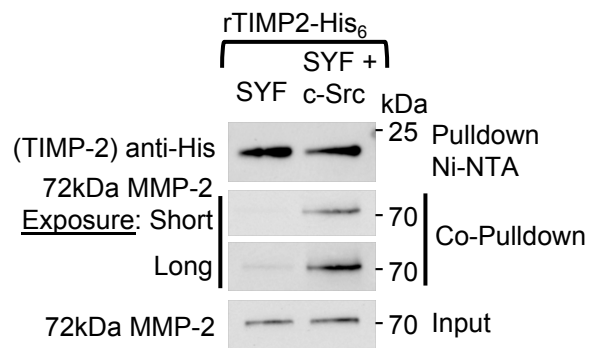
(B) and from immortalized (HEK293H and normal prostate epithelial RWPE1) or tumorigenic derivative RWPE2, human prostate tumor cell lines LNCaP, DU145 and PC3. GAPDH indicates equal cellular (extracts) protein content.

Figure S3

A CM



B CM



**Figure S3. [TIMP-2:MMP-2 interaction depends on TIMP-2 phosphorylation],
Related to Figure 3**

(A) HEK293H cells were transiently transfected with WT, TF (Y62F/Y90F/165F) and TE (Y62E/Y90E/Y165E) TIMP-2 mutants. CM were collected for pulldown and co-pulldown experiments and immunoblotted as indicated to assess interaction.

(B) SYF and SYF+c-Src cells were treated with 50ng/ml of exogenous recombinant TIMP-2-His₆ and CM were collected for immunoblotting pulldown, co-pulldown experiments.

Figure S4

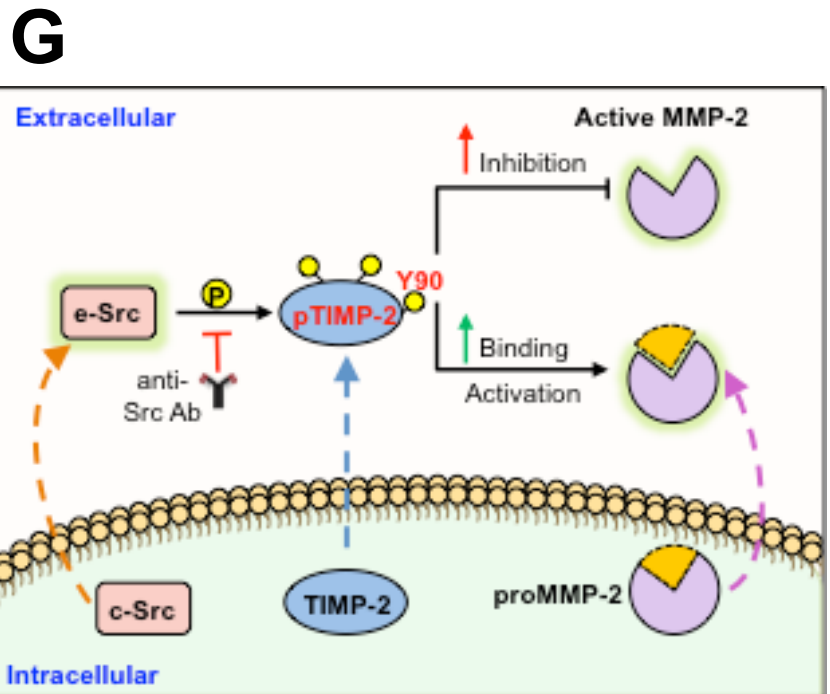
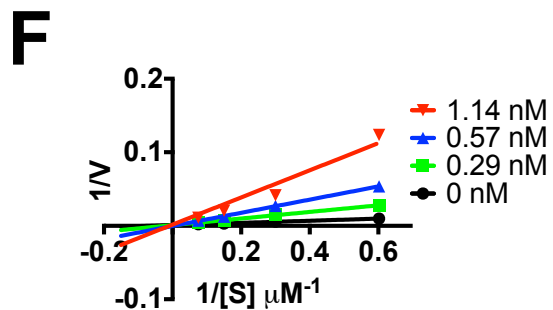
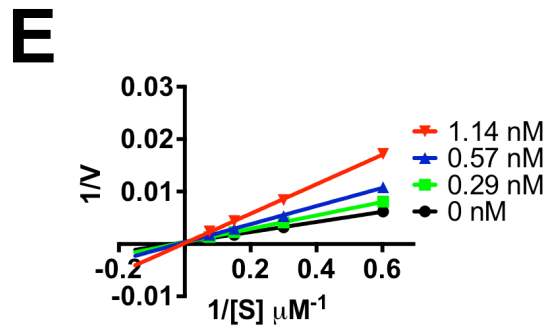
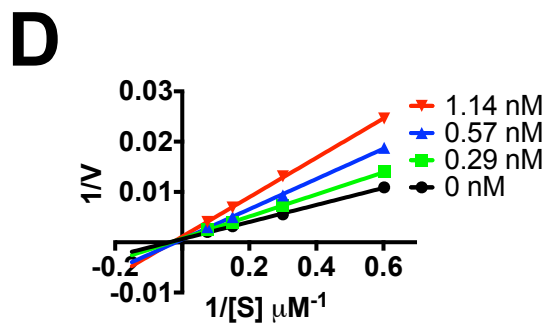
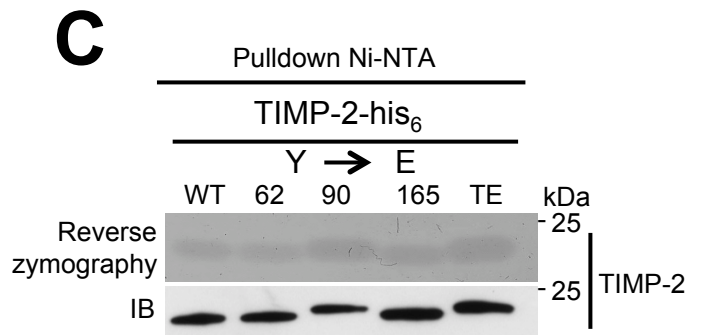
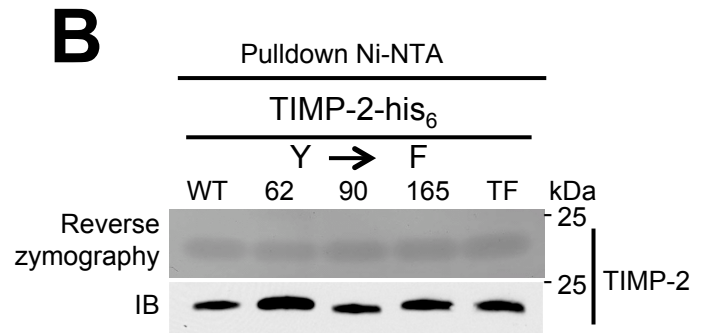
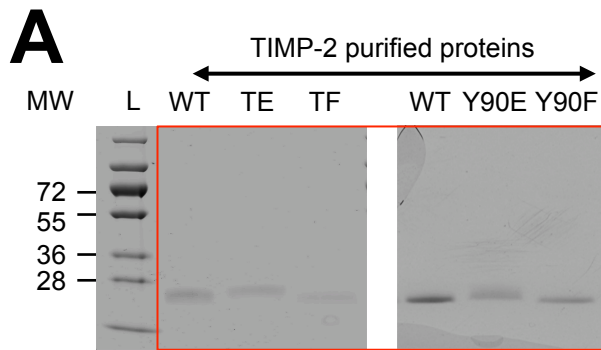


Figure S4. [TIMP-2 WT and mutant protein function and effect on MMP-2 activity], Related to Figure 4

(A) Purified WT and mutant proteins (TE, TF, Y90E and Y90F) were analyzed for purity in coomassie stained gels.

(B) Purified TIMP-2-His₆ (WT and non-phosphorylatable F mutants;

(C) or phosphomimetic E mutants, were tested for MMP-2 inhibitory activity by reverse zymography. Equal amounts of protein were analyzed by western blot (IB).

(D-F) Lineweaver-Burke plots for the inhibition of active MMP-2 by purified TIMP-2-His₆ WT (D), Y90F (E) and Y90E (F).

(G) A Model for the extracellular phosphorylation of TIMP-2 and effect on MMP-2 activity. Related to discussion.

Table S1. [Information of antibodies used], Related to Figures 1-4

Antibody	Company	Cat Number	Dilutions used
pan-phosphotyrosine (4G10)	Millipore	#05-1050	1:1,000
6x-his	Thermo Fisher Scientific	#MA1-21315	1:2,000 - 1:20,000
TIMP-2 (D18B7)	Cell Signaling	#5738	1:1,000 - 1:5,000
TIMP-2 (T2-101)	Abcam	#ab3161	1:1,000
MMP-2 (D8N9Y)	Cell Signaling	#13132	1:1,000 - 1:2,000
MMP-2	Millipore	#MAB3308	1:1,000 - 1:4,000
GAPDH	Enzo Life Sciences	#ADI-CSA-335-E	1:10,000 - 1:20,000
c-Src (36D10)	Cell Signaling	#2109	1:1,000
c-Src (L4A1)	Cell Signaling	#2110	1:1,000
c-Src (32G6) mAb1	Cell Signaling	#2123	1:1,000
c-Src (327537)	R&D Systems	MAB3389	1:1000
Mouse IgG _{2A} Isotype Control	R&D Systems	MAB003	1:1000
goat anti-mouse IgG-HRP	Santa Cruz Biotechnology	#sc-2005	1:4,000
goat anti-rabbit IgG-HRP	Santa Cruz Biotechnology	#sc-2004	1:4,000

Table S2. [Generated constructs], Related to Figure 1 and 3

Mammalian expression vectors	Generated constructs	Other names used	Number of mutated tyrosines introduced
pcDNA3.3 TOPO	TIMP-2-6xHis-wt	WT	No mutation
	TIMP-2-6xHis-Y62F	Y62F	One
	TIMP-2-6xHis-Y71F	Y71F	One
	TIMP-2-6xHis-Y90F	Y90F	One
	TIMP-2-6xHis-Y110F	Y110F	One
	TIMP-2-6xHis-Y148F	Y148F	One
	TIMP-2-6xHis-Y165F	Y165F	One
	TIMP-2-6xHis-Y204F	Y204F	One
	TIMP-2-6xHis Y62E	Y62E	One
	TIMP-2-6xHis Y90E	Y90E	One
	TIMP-2-6xHis Y165E	Y165E	One
	TIMP-2-6xHis Y62F/Y90F	Y62F/Y90F	Two
	TIMP-2-6xHis Y62F/Y165F	Y62F/Y165F	Two
	TIMP-2-6xHis Y90F/Y165F	Y90F/Y165F	Two
	TIMP-2-6xHis Y90E/Y165F	Y90E/165F	Two
	TIMP-2-6xHis- Y62F/Y90F/Y165F	Triple F (TF)	Three
	TIMP-2-6xHis- Y62E/Y90E/Y165E	Triple E (TE)	Three
	TIMP-2-6xHis- Y62F/Y90E/Y165F	Y62F/Y90E/Y165F	Three
	TIMP-2-6xHis- Y62E/Y90E/Y165F	Y62E/Y90E/Y165F	Three

Table S4. [PCR mutagenesis primer sequences], Related to Figure 3

TIMP-2 mutant	Primer sequences
TIMP-2-Y62E	Forward: 5'-GAC TCT GGA AAC GAC ATT GAG GGC AAC CCT ATC AAG AGG
	Reverse: 5'-CCT CTT GAT AGG GTT GCC CTC AAT GTC GTT TCC AGA GTC
TIMP-2-Y90E	Forward: 5'-AAG GAT ATA GAG TTT ATC GAG ACG GCC CCC TCC TCG GCA
	Reverse: 5'-TGC CGA GGA GGG GGC CGT CTC GAT AAA CTC TAT ATC CTT

Table S5. [Buffer composition], Related to Figure 4

NP40 Lysis buffer	TBST	Protein loading buffer	TIMP-2 Reconstitution buffer
0.1% or 1% NP40 (IGEPAL)	2.42g Trizma	1.25 mL Tris pH 6.8 1M	50 mM Tris pH 7.4
1 mM MgCl ₂	8g NaCl	1mL Glycerol	10 mM CaCl ₂
100 mM NaCl	1.3 mL HCl	1mL 20% SDS	150 mM NaCl
20 mM Tris pH 7.4	1 mL Tween	215µl Bromophenol blue	0.05% Brij-35 pH 7.5
20 nM sodium molybdate	1 L dH ₂ O	500µl Beta-mercaptoethanol	
1 phos stop tablet		6mL dH ₂ O	
1 protease inhibitor tablet			

TRANSPARENT METHODS

Cell culture, primers, plasmids, transfection and antibodies

Cell lines were purchased from ATCC and cultured at low passages. No authentication method was used. Experiments were performed in cell cultures maintained up to one month before they were renewed. Cell lines had been tested for mycoplasma contamination at the early stages of the experiments. All cultures were analyzed when cells reached up to 70% confluency. HEK293H, SYF, SYF+c-Src, HT1080, MCF7, MEF TIMP-2^{-/-} ras/myc, A549 were cultured in DMEM supplemented with 10% fetal bovine serum (FBS) (Invitrogen). RWPE1 and RWPE2 were cultured in Keratinocyte Serum Free Medium (K-SFM) supplemented with 2% FBS (Invitrogen). LNCaP, DU145, PC3 and H460 were cultured in RPMI supplemented with 10% FBS. MEF TIMP-2^{-/-} ras/myc was obtained from Dr Soloway (Wang et al., 2000). Wild type TIMP-2 and mutants contained a Six-Histidine (His₆) tag at their carboxyl-terminus. HEK293H cells (293H) were cultured overnight. The next day they were transfected using *TransIT-2020* Reagent (Mirus, #MIR5405) with 2 μ g plasmid DNA by manufacturer's protocol. For conditioned media (CM) collection, culture media were replaced with serum free media for an additional 24 hours. Media collected for analysis (see below). Gene synthesis, site-directed mutagenesis and sequence verification were performed by Genewiz and/or using in-house PCR: PfuUltra HotStart (Agilent Technologies) and primers (Eurofins MWG Operon). See Table S2. [Generated constructs]. Mutagenesis primers used in this study are listed in Table S4. [PCR mutagenesis primer sequences]. The following antibodies were used in this study: anti-pan-phosphotyrosine (4G10) (Millipore, #05-1050), anti-6x-His (ThermoFisher Scientific, #MA1-21315), anti-TIMP-2 (Cell Signaling, #5738 and Abcam, ab3161), anti-MMP-2 antibodies (Cell Signaling, #13132 and Millipore, #MAB3308), anti-MMP-9 (Cell Signaling, #3852), anti-GAPDH mAb (Enzo Life Sciences, #ADI-CSA-335-E), anti-c-Src (Cell Signaling, #2109, #2110, #2123), goat anti-mouse IgG-HRP (Santa Cruz Biotechnology Inc., #sc-2005) and goat anti-rabbit IgG-HRP (Santa Cruz Biotechnology Inc., #sc-2004).

Anti-c-Src antibodies for blocking experiments: rabbit anti-Src mAb1 (32G6, biotinylated) (Cell Signaling, #8077), rabbit (DA1E mAb IgG XP™ Isotype control, biotinylated) (Cell Signaling, #4096). Antibody dilution for each assay is provided in Table S1. [Information of antibodies used]. Buffer composition is shown in Table S5. [Buffer composition]. TIMP-2 sequences are provided in Table S3. [Sequences of TIMP-2 constructs].

Immunoblotting

Conditioned media were obtained 24 hours after serum starvation and treatments. Cell media were centrifuged at 1000 rpm for 5 minutes to remove any floating cells without lysing them, and supernatant from this step was used in experiments. Cell extracts were obtained by washing confluent cells with ice-cold PBS, lysing with 0.1% NP40 lysis buffer containing protease and phosphatase inhibitors (Roche) (see Table S5. [Buffer composition]), and centrifuging at 14000 rpm in a microcentrifuge at 4°C for 10 min. Protein concentrations of the resulting supernatants were determined using Bradford assay (Bio-Rad). Equal amounts of protein in 5X protein loading buffer were boiled for 5 min, loaded on 4-20% polyacrylamide gradient gels (Bio-Rad), and electrophoresis was performed in denaturing conditions. After transfer to nitrocellulose membranes (Bio-

Rad), samples were blocked in TBST (TBS + 0.1% Tweenx20) with 5% non-fat dry milk and incubated with primary antibodies at room temperature for 1-2 hours or at 4°C overnight (Table S1. [Information of antibodies used]). Blots were incubated with the appropriate HRP-conjugated secondary antibodies for 1 hour at room temperature. Bands were visualized by incubating with ECL 2 substrate (Thermo Scientific), followed by different exposures to CLASSIC X-Ray film (Research Products International Corp).

Pulldown Ni-NTA and Immunoprecipitation

Following transient transfections, equal amounts of isolated cell extract proteins were incubated with HisPur Ni-NTA Resin (ThermoScientific) for 2 hours at 4°C. Immunopellets were washed 4 times with fresh lysis buffer (20mM HEPES pH 7.0, 100mM NaCl, 1mM MgCl₂, 0.1% NP40, protease inhibitor cocktail (Roche) and PhosSTOP (Roche). Proteins bound to Ni-NTA agarose were washed with 50 mM imidazole in lysis buffer (20 mM Tris-HCl pH 7.5, 100 mM NaCl, protease inhibitor cocktail and PhosSTOP) and eluted with either 300 mM imidazole in lysis buffer or with 5x Laemmli buffer.

Pulldowns were also performed from CM concentrated ~10X using Amicon Ultra 10K centrifugal filters (Millipore) according to the manufacturer's protocol. HiPur Ni-NTA Resin was used to pulldown His₆-tagged TIMP-2 from concentrated CM. Briefly, HisPur Ni-NTA Resin was washed 3 times by vortexing resin with 0.1% NP40 lysis buffer and pipetting off supernatant. Concentrated CM was combined with washed HisPur Ni-NTA Resin, and placed on rotator at 4°C for 1 hour. Wash step was repeated 4 times with 1% NP40 buffer + 150 mM NaCl + 50 mM imidazole to reduce non-specific binding of proteins to resin. 5X protein loading buffer was added to resin and boiled for 5 minutes. Samples were created from supernatant after removing resin by centrifugation at 15000 rpm for 30 seconds. Precipitated proteins were separated by SDS-PAGE and transferred to nitrocellulose membranes. Precipitated and co-precipitated proteins were detected by immunoblotting with indicated antibodies (Table S1. [Information of antibodies used]).

Immunoprecipitation (IP) of endogenous TIMP-2 was performed by incubating CM with TIMP-2 antibody (T2-101) (or IgG control), followed by protein G agarose for 2 hours at 4°C. Immunoprecipitates were washed four times with fresh lysis buffer (20mM HEPES pH 7.0, 10mM NaCl, 1mM MgCl₂, 0.1% NP40, plus protease and phoSTOP inhibitors) and eluted with 5 x Laemmli buffer. Precipitated proteins were separated by SDS-PAGE and transferred to nitrocellulose membrane for immunoblotting. Protein inputs were detected using anti-His or anti-TIMP-2 specific antibodies. Co-immunoprecipitated proteins were also incubated with specific antibodies (Table S1. [Information of antibodies used]).

***In vitro* kinase assay**

Purified recombinant human TIMP-2-His₆ protein was incubated with 50 µl of Ni-NTA agarose (Qiagen) for 2hr. The Ni-NTA agarose beads were washed with 30mM imidazole and then incubated with 50ng of baculovirus- expressed and purified active cSrc-GST, vSrc-GST and c-Abl (SignalChem) for *in vitro* kinase assay in the presence or absence of ATP (Sigma). When necessary and after extra washes, recombinant human proMMP-2 was added. The assay was carried out in 50mM Tris-HCl (pH7.5),

10mM MgCl₂ and 0.2mM ATP, at 28°C for 15 min. The reaction was quenched by addition of an equal volume of 5xprotein loading buffer and immunoblotting was performed in denaturing conditions (as described above).

Quantification of Src kinase activity

Activity of recombinant human c-Src and v-Src was measured as described the PiPer Phosphate Assay Kit instructions for use (Life Technologies). Standard curve with linear fit line was created from 0 to 100 mM P_i final concentration reactions. 50ng of v-Src and 50, 100, and 200ng of c-Src were run in duplicate, incubated at 37°C for 1 hour with 1mM ATP as substrate. ATP turnover was calculated as mmol Pi per mol Src per minute and relative ATPase activity was calculated from those values, with the value of v-Src representing 100% activity.

Brefeldin A Treatment

HEK293H cells were seeded overnight. Cells were transiently transfected, as described above, with empty vector control or wild-type TIMP-2-His₆ DNA. After 18-20 hrs, brefeldin A (BFA) (eBioscience Inc. San Diego, CA; REF: 00-4506-51, LOT: E00021-1633) was added to the serum free media (1:1000 dilution) for a period of 12 hours, to inhibit the ER-Golgi secretion pathway. DMSO was used as a control in the non-treated cells. Both cell extracts and CM were collected for analysis (see Immunoblotting and pulldown experiments). Pulldowns were performed to assess TIMP-2 tyrosine phosphorylation.

TIMP-2 and anti-c-Src antibody treatments

For experiments related to exogenous TIMP-2 treatment and determination of extra- or intracellular phosphorylation, H1080 cells were seeded overnight, followed by serum starvation for 24 hours. Recombinant TIMP-2-His₆ (250ng/ml) was exogenously added for 2, 8 and 16 hours. Both lysates and CM were collected for immunoblot analyses. Pulldowns Ni-NTA were performed as described above to detect tyrosine phosphorylation.

For the anti-Src blocking experiments in extra- intracellular phosphorylation, serum starved HT1080 cells were treated with anti-Src mAbs or isotype IgG controls for 1 hour followed by addition of TIMP-2 at 250ng/ml for 8 hours.

For proMMP-2 activation and gelatin zymography experiments, HT1080 cells were seeded in a 96-well plate (20,000 cells per well in 100µl) for 24 hours. Media were replaced with serum free media for 24 hours followed by treatments with HEK293H-derived purified wild type TIMP-2-His₆ protein (40ng/ml) for another 24 hours. Conditioned media was collected for gelatin zymography to detect gelatinase activity. This experiment was performed three times using WT TIMP-2 from the same preparation and twice using TIMP-2 protein from different preparations. Media collected and analyzed as described (see Gelatin zymography).

Detection of c-Src in conditioned media (CM) of normal and cancer cell lines

Cell lines were cultured and serum starved for 24 hours. Cell extracts and CM were collected and processed as described above. Non-concentrated protein samples from CM were equalized to the cellular protein levels prior to immunoblotting (see above).

Protein purification of TIMP-2-His₆ WT and mutants from HEK293H conditioned media

To purify TIMP-2-His₆ mutants, we used 50 times concentrated CM from 293H cells in which the TIMP-2-His₆ WT and mutants had been transiently expressed. Precipitation pulldown protocol was followed as described before until the second wash step. After washing resin 4 times with 1% NP40 buffer + 500mM NaCl, TIMP-2 reconstitution buffer containing 0.5 M imidazole was added to resin and placed on rotator at 4°C for 1 hour (Table S5. [Buffer composition]). Samples were centrifuged at 3000 rpm for 30 seconds to release the protein and supernatant was loaded into Amicon Ultra 10K centrifugal filters (EMD Millipore). Resin was washed once with TIMP-2 reconstitution buffer (without imidazole) and this wash was also processed through Amicon Ultra 10K centrifugal filters. Purified TIMP-2-His₆ proteins were concentrated down to ~50 µl. For a second round of purification, this fraction was combined with 1% NP40 buffer + 500 mM NaCl and placed on rotator at 4°C for 15 min. Using Amicon Ultra 50K centrifugal filters (Millipore), samples were concentrated down to ~100 µl. Flow-through was kept for analysis. Concentrated sample above filter was then washed with 1% NP40 buffer + 500 mM NaCl and concentrated down to ~100 µl again. This wash step was repeated 3 times. Combined flow-through was saved and placed in Amicon Ultra 10K centrifugal filters to concentrate the purified TIMP-2-His₆ samples and remove salt from buffer. Samples were concentrated down to ~30 µl, and flow-through from this step was discarded. Buffer exchange was done by placing TIMP-2 reconstitution buffer above filter and concentrating again to yield a final volume of ~30 µl. The purity of the isolated proteins was examined by Coomassie staining of SDS-PAGE gels using GelCode Blue Safe Protein Stain (Thermo Scientific). TIMP-2 concentrations were determined using the human TIMP-2 Quantikine ELISA kit (R&D).

Gelatin Zymography

Gelatinase activity in CM was detected by gelatin zymography (Kleiner and Stetler-Stevenson, 1994). HT1080 cell cultures in 24-hour serum-free media were treated with different concentrations of purified TIMP-2 (wild type or mutants) for another 18 hours. Equal amounts of CM from HT1080 cells with and without treatments were subjected to electrophoresis using 8% acrylamide gels containing 0.1% gelatin. The gels were incubated for 30 min at room temperature in zymogram renaturing buffer (Novex, Invitrogen), 30 min at room temperature in zymogram developing buffer (Novex, Invitrogen), and then transferred to fresh zymogram developing buffer for overnight incubation at 37°C. Gels were then stained with Coomassie Brilliant Blue R-250 (Bio-Rad) and briefly destained in 10% acetic acid, 40% methanol and distilled water. They were imaged using an Epson Perfection V700 scanner. Gelatinase activity was detected as transparent bands on a dark background. Recombinant human proMMP-2 was run alongside CM as a control to confirm the identity of MMP-2 in the samples. At least two independent proMMP-2 activation experiments were performed using proteins prepared from different purifications for treatment.

Reverse Zymography

Reverse gelatin zymography was performed to test WT and mutant TIMP-2 proteins inhibitory function towards MMP-2. Equal amounts (1ng) of purified TIMP-2-His₆ (WT and mutants) were run in 15% acrylamide gels containing 0.225% gelatin (Sigma) and 50 ng/ml recombinant proMMP-2. The gels were incubated for 2 hours at room temperature in zymogram renaturing buffer, 30 min at room temperature in zymogram developing buffer, and then transferred to fresh zymogram developing buffer for overnight incubation at 37°C. Gels were stained and imaged as described in gelatin zymography. TIMP-2 inhibitory activity was detected as dark positive staining bands over a clear background. Recombinant human TIMP-2 (Abcam) was run alongside purified TIMP-2-His₆ mutants as a positive control.

Active MMP-2 enzyme kinetic assays

Different concentrations of an MMP-2 substrate fluorescence peptide Dabcyl-GLGMRGK(FAM)-NH₂ (1.66-13.32 μM) were titrated against active MMP-2 (62kDa MMP-2) in the presence of different concentrations of TIMP-2 WT or mutants Y90E and Y90F (0-1.14 nM) proteins. 62kDa MMP-2 was diluted in 50mM Tris pH 7.4, 2mM CaCl₂, 150mM NaCl, 5μM ZnSO₄ and 0.01% Brij-35. 50μL of each sample was then added to the 96-well assay plate and incubated for 15 minutes at room temperature. Fluorescent peptide was subsequently added to the plate at a volume of 50μL. Fluorometric analysis was performed at excitation of 485 and emission of 530nm. Fluorescence measurements were taken for 1 hour, at 5 minutes intervals. The initial velocities of the reaction were determined for each measurement. The rate of reaction was then plotted in relation to the amount of substrate and concentration of inhibitor. Following this, Michaelis-Menten and Lineweaver Burk Plots were produced through GraphPad Prism version 7.00 for Windows, GraphPad Software, La Jolla California USA, www.graphpad.com. Km apparent values were determined for each of the inhibitor concentrations and using a rearrangement of the classic competitive inhibition formula, $-1/Km(app) = -1/(Km(1 + [I]/K_i))$, K_i was produced for each individual TIMP-2 protein. A simple Student's *t*-test was used to calculate significance levels between the replicates of the experiments. The significance of the sample was marked with a *, $P < 0.05 = *$, $P < 0.01 = **$, $P < 0.001 = ***$. Error bars correspond to s.e.m+ s.d. from two to three technical replicates. Two experimental replicates using protein purifications from different preparations were performed. Measurements were taken using SpectraMaxi3 (Molecular Devices).

Statistical analysis

No statistical methods were used to predetermine sample size. *P* values for MMP-2 enzymatic activity assay were calculated using unpaired two-tailed Student's *t*-tests with Welch's correction for unequal SDs when two groups were compared (GraphPad Prism 6). *P* values with asterisk indicate significance. In the experiments, *n* represents the number of technical replicates. The overall presented experiments in the manuscript are representative of minimum two, generally three biological replicates. Molecular graphics and analyses were performed with the UCSF Chimera package. Chimera is developed by the Resource for Biocomputing, Visualization, and Informatics at the University of California, San Francisco.

Supplemental References

Kleiner, D.E., and Stetler-Stevenson, W.G. (1994). Quantitative zymography: detection of picogram quantities of gelatinases. *Anal Biochem* 218, 325-329.